Figure S1: Schematic representations and analytical restriction digestions of the plasmid DNA constructs used for the quadruple mutant (ΔQ) generation. (A1 to D1) Partial schematic representations of (A) pSLR1106KAN, (B) pSLR1768CAM, (C) pSLR1128SPEC and (D) pSLL0815ERM are not to scale. Target genes are represented by yellow arrows and annotated, while the flanking regions of the pBluescript II KS(+) (pBS) or the pGEM-T easy vectors are indicated by dashed lines. Primer (represented by arrows underneath) introduced restriction sites are marked in black. Restriction sites used for antibiotic-resistance cassette insertion (KAN^R, CAM^R, $SPEC^R$ and ERM^R; marked in green; direction of transcription indicated by white arrow) are marked in red. (A1) The *slr1106* gene (849 bp) was disrupted by a kanamycin-resistance cassette (KAN^R; 1.25 kb) that was inserted at the NaeI site at position 236 of the gene. (B) The *slr1768* gene (897 bp) was disrupted by a chloramphenicol-resistance cassette (CAM^R; 1.3 kb) that was inserted at the EcoNI site at position 265 of the gene. (C) The *slr1128* gene (966 bp) was disrupted by a spectinomycin-resistance cassette ($SPEC^R$; 2.07 kb) inserted at the MscI site at position 238 of the gene. (D) The *sll0815* gene (795 bp) was disrupted by an erythromycin-resistance cassette (ERM^R; 1.54 kb) inserted at the HindIII site at position 458 of the gene. DNA fragment lengths (in kb) in between the respective restriction sites are indicated underneath. (A2 to D2) Analytical restriction digestions on the respective plasmid DNA constructs with indicated restriction enzymes.

Figure S2: PCR analysis and schematic depiction of the Band 7 gene regions in the quadruple mutant (ΔQ*) strain. The following genes were inactivated by directed mutagenesis in the quadruple mutant strain (ΔQ*): *slr1106*, *slr1768*, *slr1128* and *sll1021* (see also Fig. S1). (A) Complete segregation was confirmed by PCR analysis using specific primers and genomic DNA isolated from the Synechocystis sp. PCC 6803 GT and quadruple mutant (ΔQ*) strains. (B to F) Schematic depictions of the Band 7 gene regions in the quadruple mutant strain. The primers

used to amplify the Band 7 gene regions and the sizes of respective fragments are indicated. Drawings are not to scale. Kanamycin-resistance cassette (KAN^R), chloramphenicol-resistance cassette (CAM^R), spectinomycin-resistance cassette ($SPEC^R$) and erythromycin-resistance cassette (ERM^R).

Figure S3: Electron micrographs of cells of *Synechocystis* sp. PCC 6803 GT and quadruple mutant ∆Q. Electron micrographs of ultra-thin sections of (A1 to A3) *Synechocystis* sp. PCC 6803 wild-type GT and (B1 to B3) quadruple mutant (ΔQ) cells were taken at a magnification of (A1 and B1) 13.000x and (A2 and B2) 28.500x. (A3 and B3) A GT and a quadruple mutant cell (marked with large grey arrows in A2 and B1) were further magnified *in silico*. Some dividing cells are marked (small grey arrows). The following inclusions are also marked: Thylakoid membrane (large white arrow), carboxysome (small white arrow), polyhydroxyalkanoate (PHA) granule (large black arrow) and polyphosphate body (small black arrow). The scale bars represent 1 µm, as indicated.

Figure S4: Cell motility of the *Synechocystis* sp. PCC 6803 wild-type and various single Band 7 gene inactivation mutant strains. Cell motility was assessed in a plate assay with 10-µl aliquots of liquid cell cultures (diluted to an OD_{730} of 0.1) spotted onto BG-11 1.5 % (w/v) agar plates and incubated under diffuse light (15 µE m^{-2} s^{-1}). Droplets were photographed after 10 days and the extents of the droplets at the start of the experiment are indicated by white circles.

Figure S5: Photoinhibition analysis of the *Synechocystis* sp. PCC 6803 wild-type GT and the ΔQ quadruple mutant. Cells at a chl *a* concentration of 20 µg ml^{-1} were high-light treated (1200 µE m^{-2} s^{-1}) at 29 °C over a period of six hours. Oxygen evolution of whole cells was assessed for the *Synechocystis* sp. PCC 6803 wild-type GT (black lines) and the ΔQ quadruple mutant (red line) strains in the presence (closed symbols) or absence (open symbols) of 100 µg ml^{-1}

lincomycin at the indicated time points in the presence of 2 mM 2,6 dichlorobenzoquinone (DCBQ) and 1 mM $K_3Fe(CN)$ using a Hansatech DW2 oxygen electrode (Hansatech instruments Ltd., UK). Oxygen evolution rates (µmol oxygen mg chl *a* $^{-1}$ h^{-1}) were normalised (value at t=0 was 100 %) and plotted as a function of time. Error bars represent standard deviation from the mean of three measurements. The initial, absolute rates of oxygen evolution for the respective strains were: 324 (ΔQ -Linc), 316 (GT -Linc) and 350 (GT +Linc) (all in µmol oxygen mg chl *a* $^{-1}$ h^{-1}).

Figure S6: Comparative pulse-chase analysis of the *Synechocystis* sp. PCC 6803 GT and the quadruple mutant strains. Crude membranes were isolated from (A) *Synechocystis* sp. PCC 6803 GT and (B) quadruple mutant aliquots taken after a pulse period and at chase time points (0, 45, 90 and 180 min). (A1 and B1) Membrane samples containing 1 µg of chl *a* were separated on 1-D SDS PAGE gels that were used to generate autoradiograms. Autoradiograms were developed using a Phosphorimager reader (Fuji Film Scanner FLA-5000, Fuji, UK) and the D1 protein signal is indicated (arrow). (A2 and B2) D1 signals were quantified using AIDA software (version 3.28) and plotted as percentage of signal intensity compared to t = 0.

Figure S7: Immunoprecipitation experiment on crude membrane isolation of various *Synechocystis* sp. PCC 6803 strains using the αNdhI, αNdhJ and αSlr1106 antibodies. Crude membrane isolations of the *Synechocystis* sp. PCC 6803 GT, the ΔQ quadruple mutant and the M55 strain (ΔNdhB) were used in an immunoprecipitation experiment with the indicated antibodies (αSlr1106, αNdhI and αNdhJ). 15 µl of the immunoprecipitations (the samples had been eluted in 70 µl 1x SDS sample buffer) were loaded in the respective lanes. (A1) One 1-D SDS PAGE gel was Coomassie-stained, while (A2) another was used for an immunoblotting analysis with the αSlr1106 antibody.

Figure S8: Comparative 2-D BN/SDS PAGE analysis of the *Synechocystis* sp. PCC 6803 GT and the ΔQ quadruple mutant strains under different CO_2 growth conditions. Crude membranes of (A) the *Synechocystis* sp. PCC 6803 GT and (B) the ΔQ quadruple mutant strains were isolated and separated by 2-D BN/SDS PAGE. Cells were grown under standard laboratory growth conditions, except for a change in the pH of the liquid BG-11 media (pH = 7.5 instead of 8.2) and different CO_2 conditions. The CO_2 conditions under which the liquid cultures were grown were as follows: (A1 and B1) at high CO_2 (3 % (v/v) CO_2 in air), (A2 and B2) at low CO_2 (air level) and (A3 and B3) with a shift from high CO_2 (3 % (v/v) CO_2 in air) to low CO_2 (air level). An amount of crude isolated membranes corresponding to 5 µg chl *a* were separated in each lane of a 5 to 12.5 % (w/v) linear gradient BN PAGE gel. The gel strips for the second dimension SDS PAGE gels were incubated for 1 h in solubilisation buffer, transferred and run on 14 % SDS PAGE gels that were subsequently silver-stained. The positions of various protein complexes are indicated with arrows. Protein complexes that were induced by the change of the CO2 level, are indicated in grey. The position of the Slr1128 protein is marked with a grey circle.

Figure S9: Immunoprecipitation of the Slr1128 protein of *Synechocystis* sp. PCC 6803. A crude membrane isolation of a high light induced *Synechocystis* sp. PCC 6803 GT strain (exposed to an illumination of 1000 µE m^{-2} s^{-1} for 1 h to induce the Hli proteins) was used for an immunoprecipitation analysis (the initial sample contained 40 µg of chl *a*) with αSlr1128 purified antibody-coupled to Protein A sepharose beads and Protein A sepharose beads without coupled antibody. A crude GT membrane sample (2 µg of Chl *a*) and the eluted fractions (15 µl of a total volume of 80 µl; eluted in 1x SDS buffer) were analysed by (A) 1-D SDS PAGE and (B and C) immunoblotted with antibodies directed against the HliA (Ssl2542, also termed ScpC, it also recognizes Ssr2595 termed HliB or ScpD) and the HliD (Ssr1789, also termed ScpE) proteins. The arrow indicates the position of the immunoprecipitated Slr1128 protein.

Figure S10: Affinity-purification of His_6-tagged CP47 protein. The samples of a Ni-NTA magnetic beads affinity-purification of His_6-tagged CP47 protein from the CP47-His/TD41 and TD41 (control) *Synechocystis* sp. PCC 6803 strains were analysed by 1-D SDS PAGE and immunoblotting. TD41 is a *psbA*-triple deletion strain unable to synthesise D1. The pre- and postbinding samples corresponded to an amount of 1 µg Chl *a*, while only 7.5 µl of the 500 µl washing (100 mM Imidazole) and elution fractions (250 and 500 mM Imidazole) were loaded. One gel was (A) silver-stained or (B to F) used for immunoblots with the indicated antibodies.

Figure S1

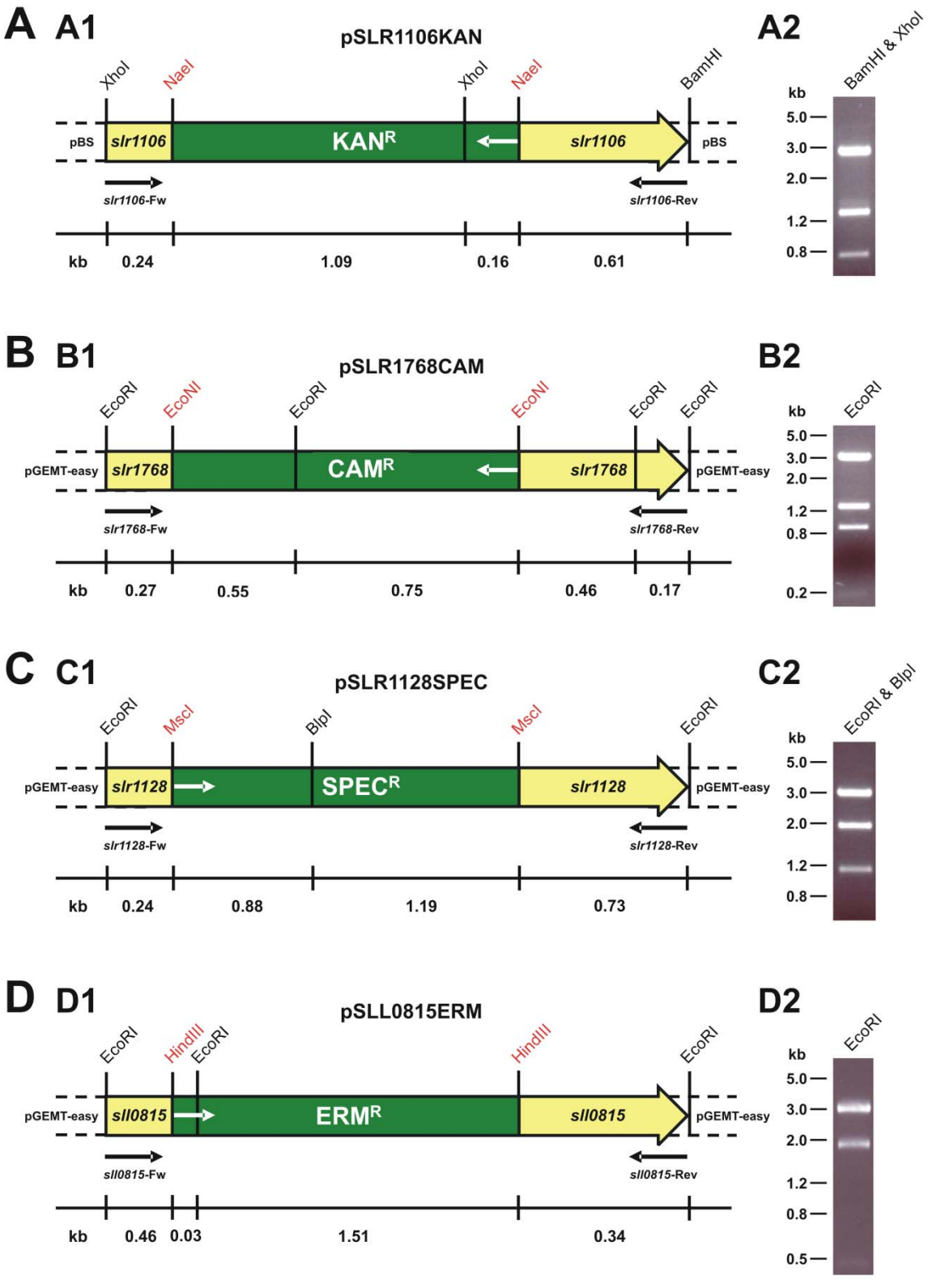
A
A1
pSLR1106KAN
XhoI
NaeI
XhoI
NaeI
BamHI
pBS
slr1106
KAN^R
slr1106
pBS
slr1106-Fw
slr1106-Rev
kb
0.24
1.09
0.16
0.61
A2
BamHI & XhoI
kb
5.0
3.0
2.0
1.2
0.8
B
B1
pSLR1768CAM
EcoRI
EcoNI
EcoRI
EcoNI
EcoRI
EcoRI
pGEMT-easy
slr1768
CAM^R
slr1768
pGEMT-easy
slr1768-Fw
slr1768-Rev
kb
0.27
0.55
0.75
0.46
0.17
B2
EcoRI
kb
5.0
3.0
2.0
1.2
0.8
0.2
C
C1
pSLR1128SPEC
EcoRI
MscI
BlpI
MscI
EcoRI
pGEMT-easy
slr1128
SPEC^R
slr1128
pGEMT-easy
slr1128-Fw
slr1128-Rev
kb
0.24
0.88
1.19
0.73
C2
EcoRI & BlpI
kb
5.0
3.0
2.0
1.2
0.8
D
D1
pSLL0815ERM
EcoRI
HindIII
EcoRI
HindIII
EcoRI
pGEMT-easy
sll0815
ERM^R
sll0815
pGEMT-easy
sll0815-Fw
sll0815-Rev
kb
0.46
0.03
1.51
0.34
D2
EcoRI
kb
5.0
3.0
2.0
1.2
0.8
0.5

Figure S2

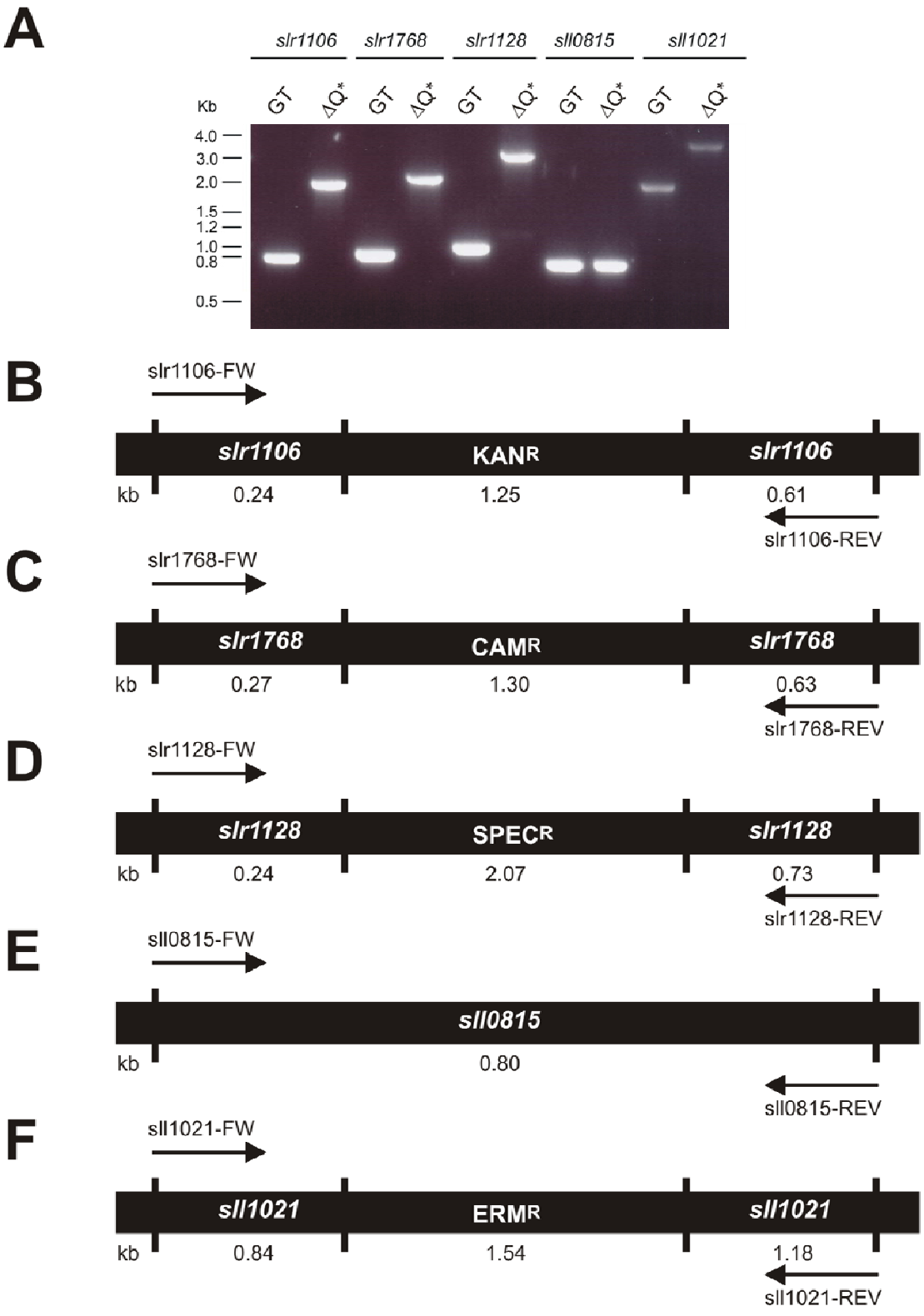
A
slr1106
slr1768
slr1128
sll0815
sll1021
Kb
GT
ΔQ*
4.0
3.0
2.0
1.5
1.2
1.0
0.8
0.5
B
slr1106-FW
slr1106
KANR
slr1106
kb
0.24
1.25
0.61
slr1106-REV
C
slr1768-FW
slr1768
CAMR
slr1768
kb
0.27
1.30
0.63
slr1768-REV
D
slr1128-FW
slr1128
SPECR
slr1128
kb
0.24
2.07
0.73
slr1128-REV
E
sll0815-FW
sll0815
kb
0.80
sll0815-REV
F
sll1021-FW
sll1021
ERMR
sll1021
kb
0.84
1.54
1.18
sll1021-REV

Figure S3

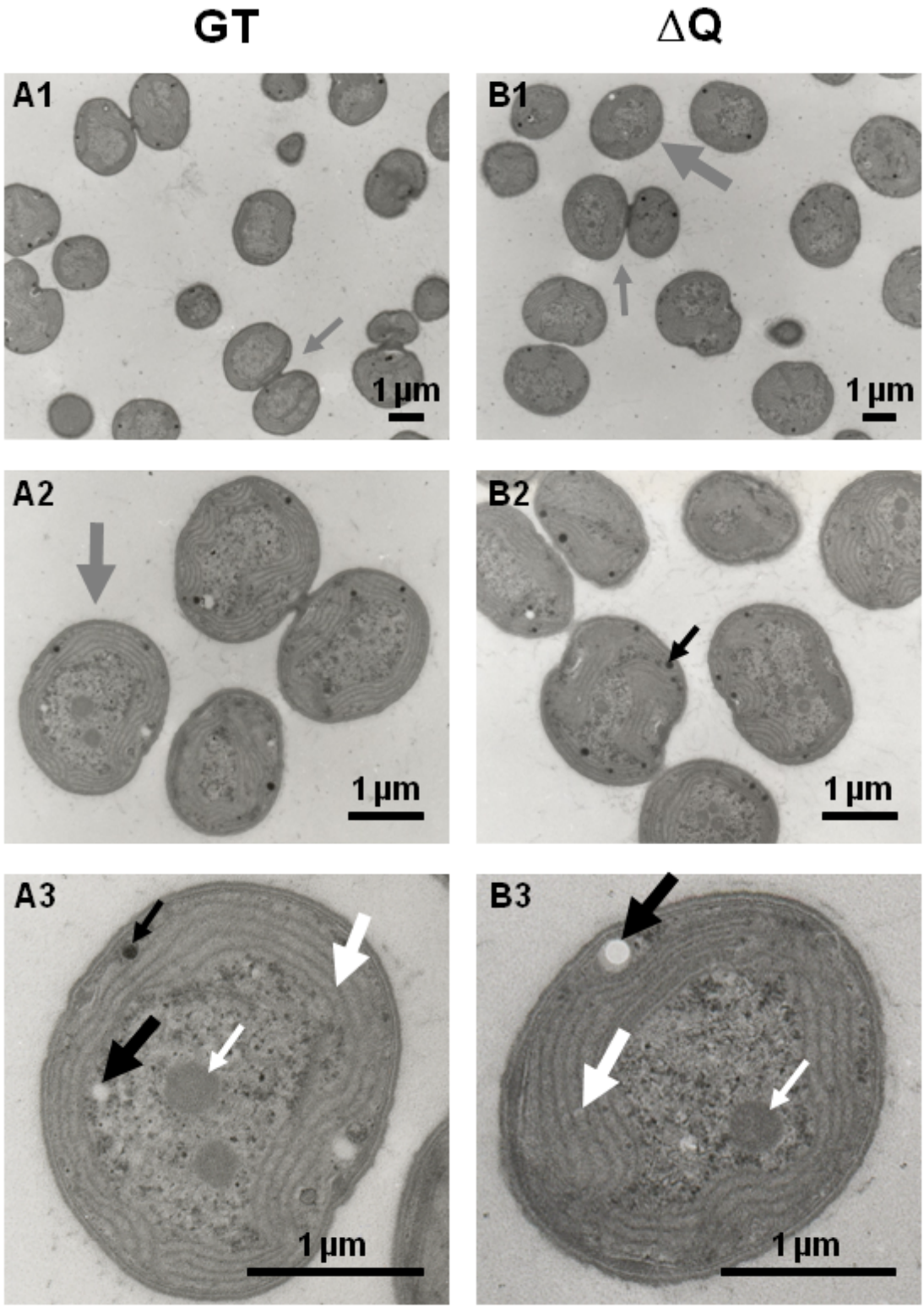

Figure S4

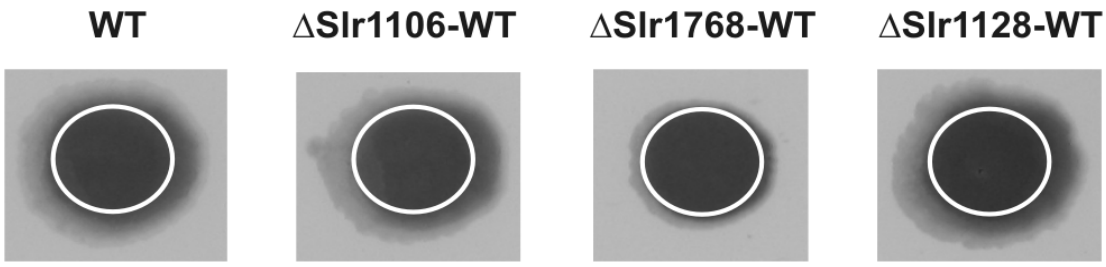

Figure S5

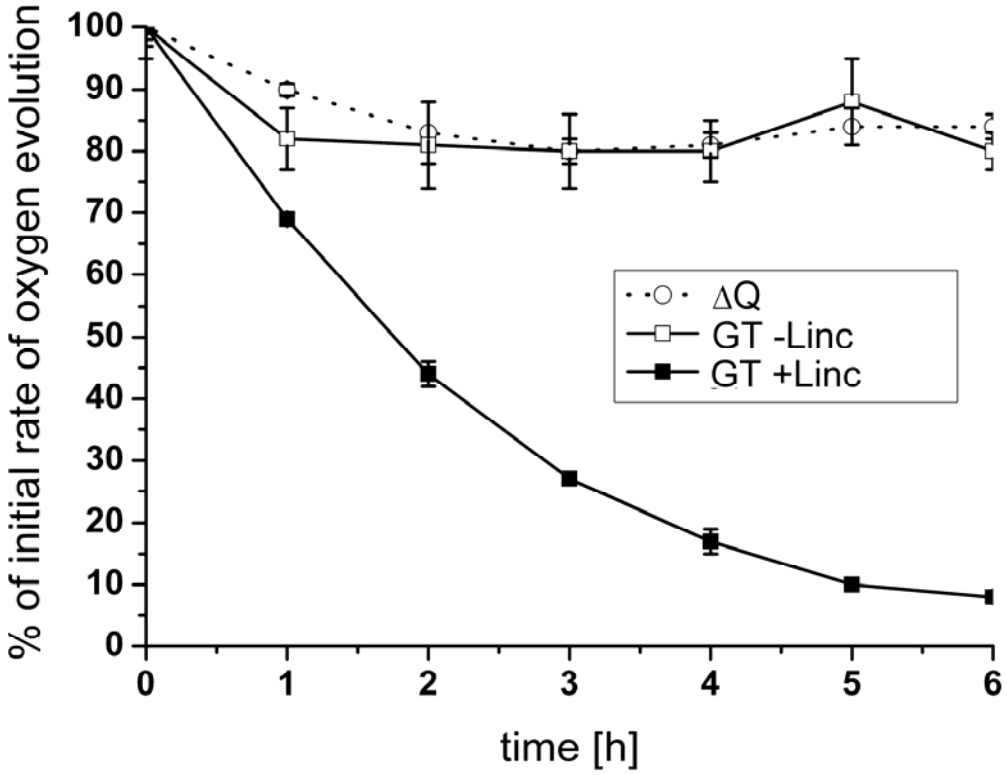
% of initial rate of oxygen evolution
100
90
80
70
60
50
40
30
20
10
0
0
1
2
3
4
5
6
time [h]
ΔQ
GT -Linc
GT +Linc

Figure S6

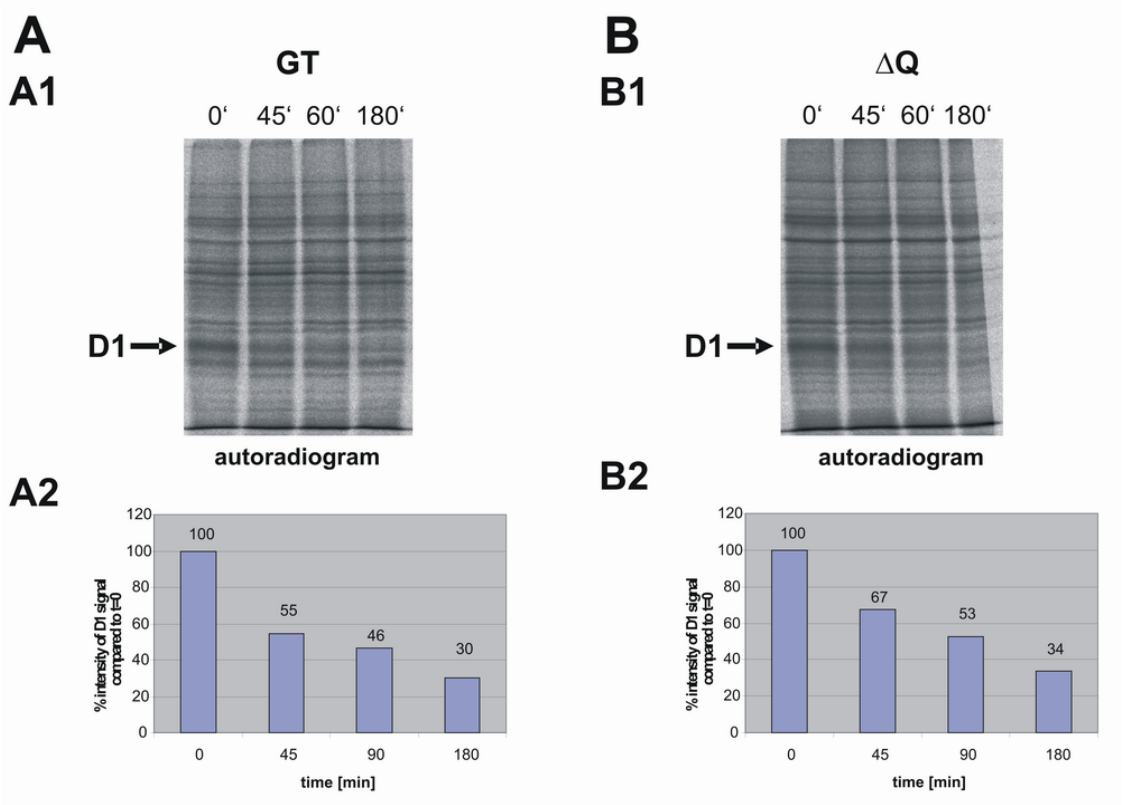
A
A1
GT
0‘ 45‘ 60‘ 180‘
D1
autoradiogram
A2
% intensity of D1 signal compared to t=0
100
55
46
30
time [min]
B
B1
ΔQ
0‘ 45‘ 60‘ 180‘
D1
autoradiogram
B2
% intensity of D1 signal compared to t=0
100
67
53
34
time [min]

Figure S7

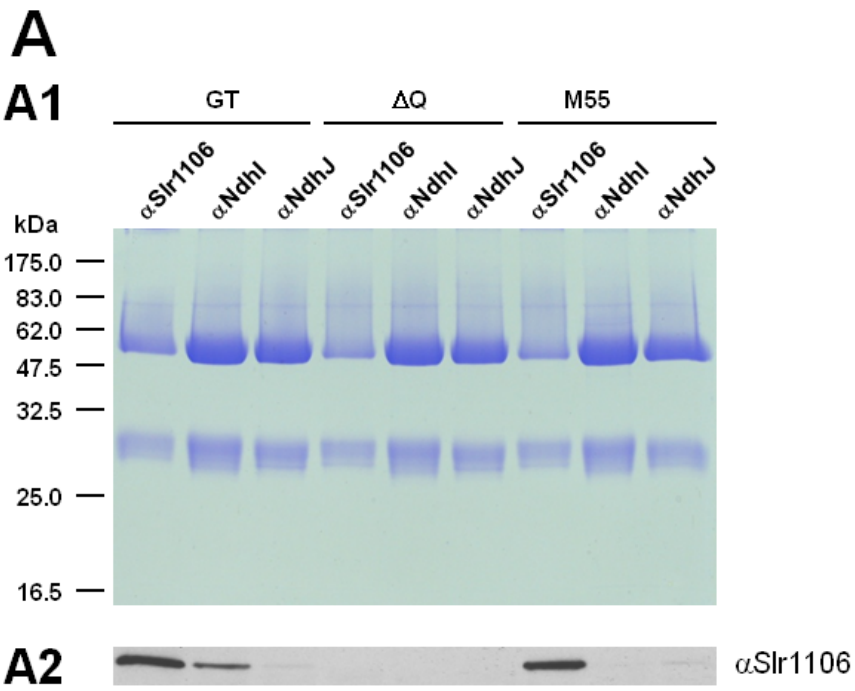
A
A1
GT
ΔQ
M55
αSlr1106
αNdhI
αNdhJ
αSlr1106
αNdhI
αNdhJ
αSlr1106
αNdhI
αNdhJ
kDa
175.0
83.0
62.0
47.5
32.5
25.0
16.5
A2
αSlr1106

Figure S8

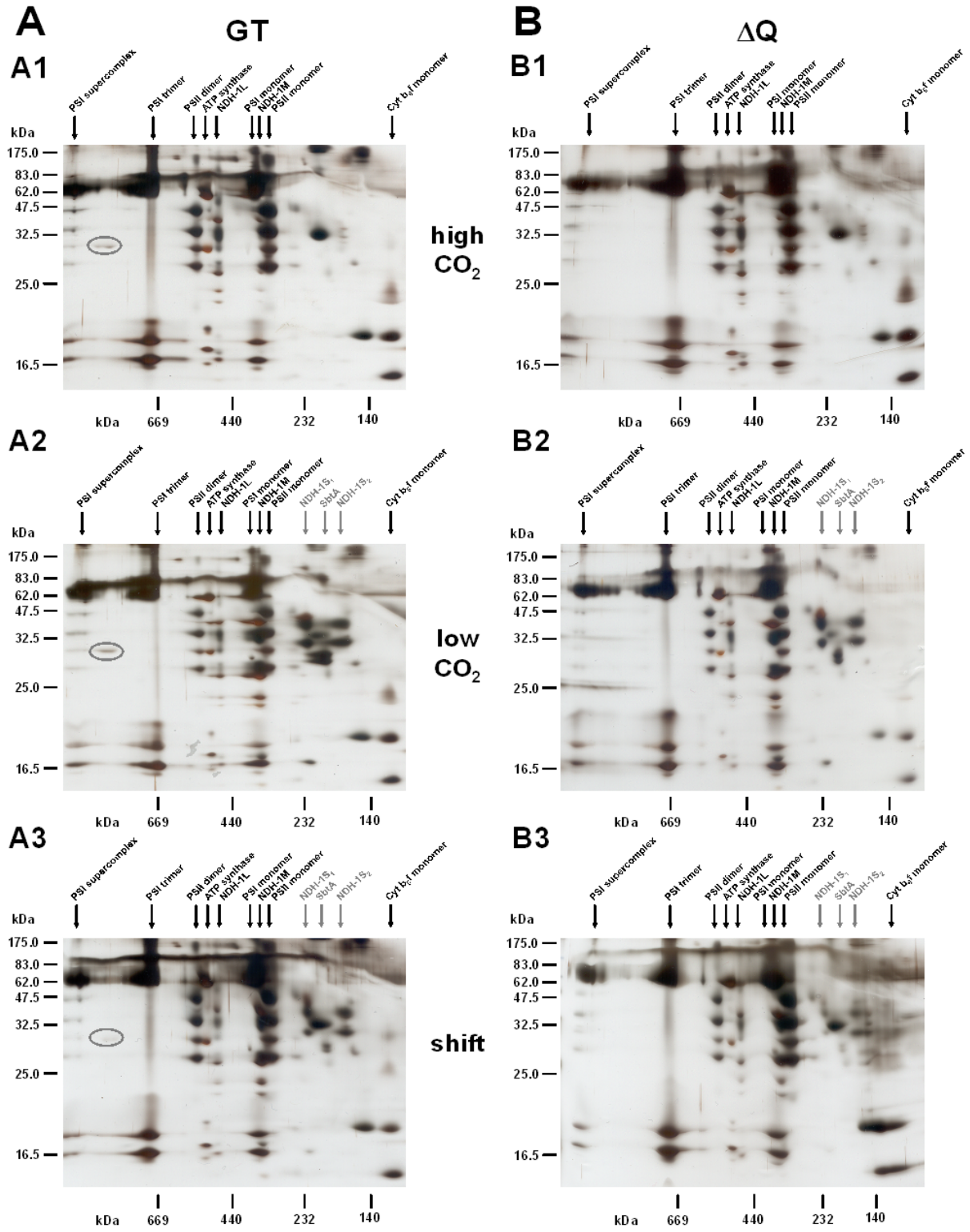
A
GT
A1
PSI supercomplex
PSI trimer
PSII dimer
ATP synthase
NDH-1L
PSI monomer
NDH-1M
PSII monomer
Cyt b6f monomer
kDa
175.0
83.0
62.0
47.5
32.5
25.0
16.5
669
440
232
140
high CO2
A2
NDH-1S1
StbA
NDH-1S2
low CO2
A3
shift
B
ΔQ
B1
B2
B3

Figure S9

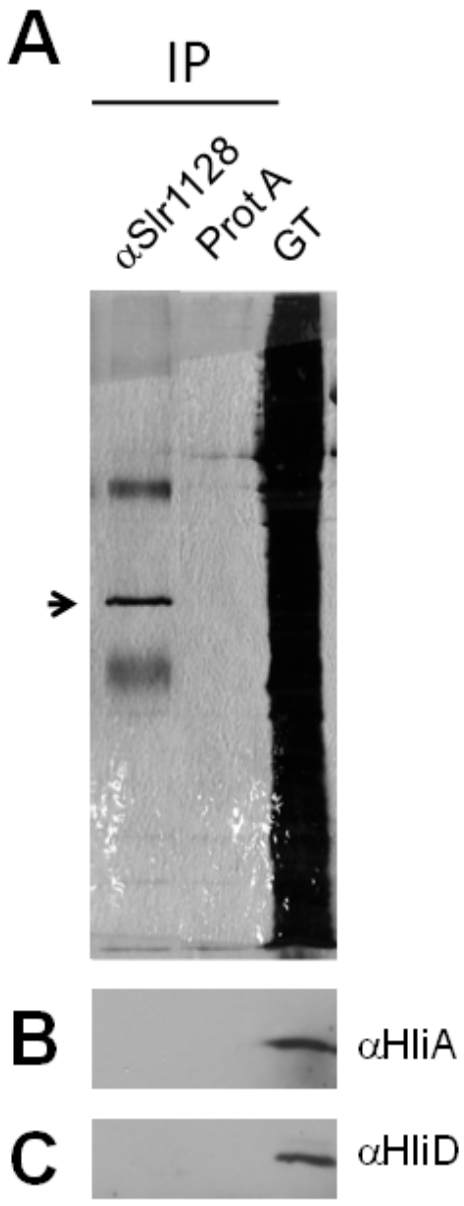

Figure S10

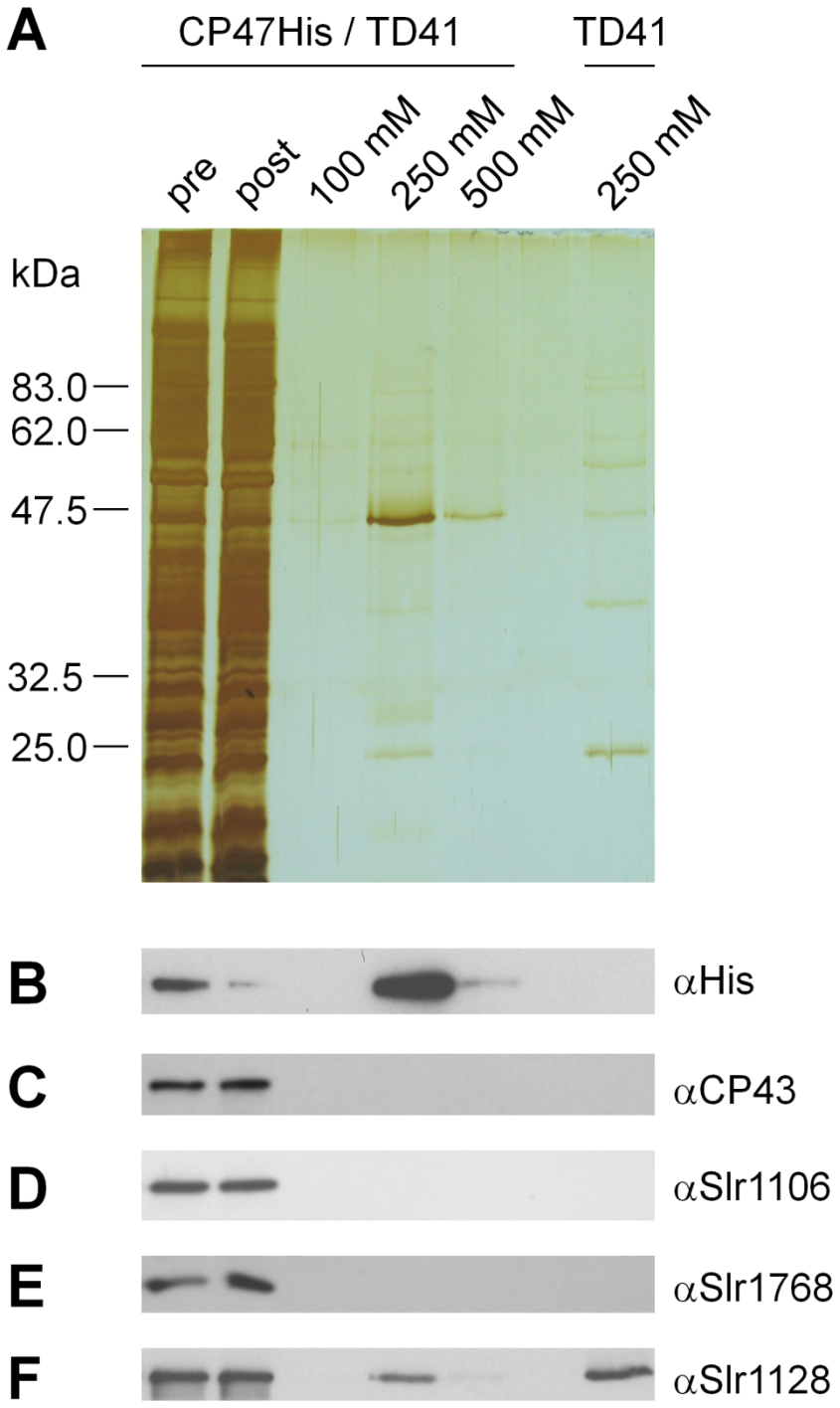
A
CP47His / TD41
TD41
pre
post
100 mM
250 mM
500 mM
250 mM
kDa
83.0
62.0
47.5
32.5
25.0
B
αHis
C
αCP43
D
αSlr1106
E
αSlr1768
F
αSlr1128